ISSN 1027-5495. Functional Materials, 28, No.4 (2021), p. 652-661.
doi:https://doi.org/10.15407/fm28.04.652

Effects of grain-size and specimen thickness on dislocation kinetics in uniaxially strained thin Al sheets with one grain in thickness

Ye.V.Ftomov, O.V.Shekhovtsov, E.E.Badiyan, A.G.Tonkopryad

V.Karazin Kharkiv National University, 4 Svobody Sq.,
61022 Kharkiv, Ukraine

Received September 22, 2021

This study expands the well-known Kocks-Mecking strain hardening model by describing the effects of grain size and sample thickness, as well as the kinetics of dislocations during uniaxial deformation of thin aluminum sheets with one grain in thickness. In the kinetic equation for the dislocation density, the coefficients are determined for the case of flat samples with a "pancake" grain structure. The kinetic equation was transformed using Taylor's law of strain hardening in a standard way; and the solution to this equation was obtained to calculate the stress — strain curve of Al specimens with average grain sizes and thicknesses in the range of $0.2 < d_s < 20$ mm and $0.05 < t < 1$ mm, respectively. An approximate Hall-Petch type relation is obtained. Based on the kinetic consideration of the processes of storage and recovery of dislocations, the effect of the grain size and specimen thickness on the flow stress and the strain-hardening rate is studied. The calculation results are in good agreement with obtained experimental data.

Keywords: uniaxial straining, dislocation kinetics, thin Al sheets, "pancake" grain structure.

Ефекти впливу розміру зерен і товщини зразка на дислокаційну кінетику при одноосьовому розтягуванні тонких алюмінієвих пластин з одним шаром зерен за товщиною. *Є.В.Фтьомов, О.В.Шеховцов, Є.Ю.Бадіян, А.Г.Тонкопряд*

Проведене дослідження показало, що відома Kocks-Mecking модель деформаційного зміцнення для опису дислокаційної кінетики та ефектів впливу розміру зерен і товщини зразка при одноосьовому розтягуванні тонких алюмінієвих пластин з одним шаром зерен за товщиною отримала подальший розвиток. У кінетичному рівнянні для густини дислокацій визначено коефіцієнти у випадку плоских зразків із "млинцевою" зеренною структурою. Кінетичне рівняння перетворено у стандартний спосіб із використанням закону деформаційного зміцнення Тейлора й отримано розв'язок цього рівняння для розрахунку кривої "напруження-деформація" алюмінієвих зразків із середніми розмірами зерен і товщинами в інтервалах $0.2 < d_s < 20$ мм і $0.05 < t < 1$ мм відповідно. Одержано апроксимаційне співвідношення, яке є аналогічним співвідношенню Холла-Петча. На підставі кінетичного розгляду процесів накопичення та зникнення дислокацій досліджено вплив розміру зерен і товщини зразка на напруження плину та коефіцієнт деформаційного зміцнення. Зіставлення результатів розрахунків з одержаними експериментальними даними свідчить про їхню добру узгодженість.

Получила дальнейшее развитие известная Kocks-Mecking модель деформационного упрочнения для описания дислокационной кинетики и эффектов влияния размера зерен и толщины образца при одноосном растяжении тонких алюминиевых пластин с одним слоем зерен по толщине. В кинетическом уравнении для плотности дислокаций определены коэффициенты в случае плоских образцов с "блинной" зеренной структурой. Кинетическое уравнение преобразовано с использованием закона деформационного

упрочнения Тейлора стандартным образом и получено решение этого уравнения для расчета кривой "напряжение-деформация" алюминиевых образцов со средними размерами зерен и толщинами в интервалах $0.2 < d_s < 20$ мм и $0.05 < t < 1$ мм соответственно. Получено аппроксимационное соотношение, аналогичное соотношению Холла-Петча. На основе кинетического рассмотрения процессов накопления и исчезновения дислокаций исследовано влияние размера зерен и толщины образца на напряжение течения и коэффициент деформационного упрочнения. Сопоставление результатов расчета с полученными экспериментальными данными свидетельствует об их хорошем согласовании.

1. Introduction

Polycrystalline metals are widely used for the fabrication of tools and for supporting structures. The mechanical properties and deformation mechanisms of bulk metal are well known. Recently, micro- and nanocrystalline materials have been used in the medical industry, microelectronics, and nanotechnology. Thin films, foils and plates with a several grains across thickness are processed and examined [1–6].

The mechanical behavior of thin sheets is sensitive not only to microstructure. The mechanical properties of thin specimens depend on the grain size d and the thickness t. It is well known that fine-grained metals are stronger than coarse-grained metals due to the influence of grain boundaries on the accumulation of dislocations. In particular, the Hall-Petch relation describes the dependence of initial yield strength on grain size [7, 8]. On the other hand, the experimental results showed that the flow stress decreases with decreasing sample thickness, when the number of grains in thickness becomes less than the critical value. The critical thickness increases with both a decrease in the grain size and a decrease in the stacking fault energy [9]. In [2], the mechanical behavior under uniaxial tension of 99.999 at.% Al polycrystalline sheets of various thicknesses in the range of 100–340 μm and an average grain size from 75 to 480 μm was experimentally investigated. For specimens with $1 < t/d_s < 3$ (d_s is the average grain size measured on the specimen surface), the flow stress increases significantly with increasing t/d_s. For $0.4 < t/d_s < 1$, there is a slight increase in the flow stress. For $t/d_s < 1$, the flow stress depends only on t/d_s and not on the absolute thickness or average grain size, while for $t/d_s > 1$ there is a dependence on the grain size.

Since changes in properties occur due to changes in structure, models in materials science must be based on the relationship between structure and properties. The theory of work hardening is expressed by differential equations; while their integrals give stress-strain curves $\sigma(\varepsilon)$ [10–12]. Dislocation movement causes the plastic deformation. A widely used concept of the theory of plasticity is that the flow stress σ depends on the structure changing with strain ε, and the dislocation structure can be represented by the single parameter ρ, the dislocation density. It is assumed that, at given ρ, the flow stress σ depends on the strain rate $\dot{\varepsilon}$ and temperature T [10]. At low and medium temperatures, the kinetics of hardening is determined by stress-induced slip processes that control both the accumulation of dislocations and their mutual annihilation [12].

Equations for dislocation density evolution developed for bulk metals must be corrected for thin films, foils and plates. In [13], the dislocation-kinetic approach is used to describe uniaxial straining at a medium temperature and a constant strain rate for flat plate polycrystalline specimens of pure metals with a thickness and average grain size in the range from ~ 50 μm to macroscopic values. The features of plate specimens were taken into account, such as the effect of strain hardening by "vertical" grain boundaries (see 3.2.2) in the grains of the surface layer and the role of the free surface as a source and sink for dislocations. In this article, the model is modified for thin sheets with one grain in thickness. The aim of this work is to use the dislocation-kinetic approach to study the effects of grain size and thickness in Al plates with two-dimensional pancake-shaped crystals in uniaxial tension experiments at room temperature and constant strain rate.

2. Experimental

A material with high stacking fault energy is preferred because this hampers the formation of twins which absence gives a simpler microstructure [2]. FCC metals are considered suitable as having many active well defined slip systems [2, 14]. Their uniaxial straining is generally well studied. For these reasons, we used pure aluminum (99.96 %) as an FCC metal with high stacking fault energy.

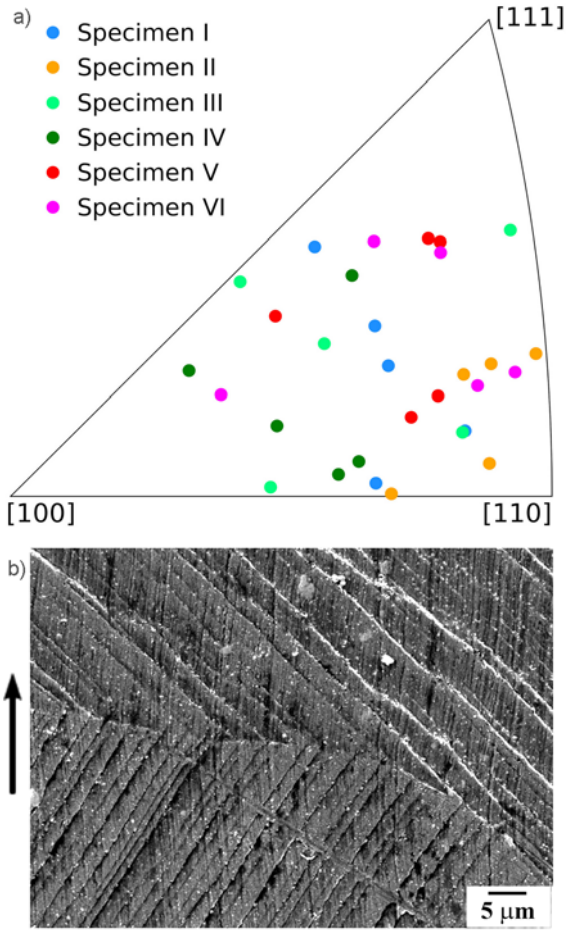

Fig. 1. Typical crystallographic orientation of grains (a) and typical slip pattern (b) in the tensile specimens.

The specimens were processed by preliminary uniaxial straining and recrystallization. Strips with a square cross section of 20 mm×0.2 mm and a width of 100 mm were cut from the aluminum foil, parallel to the original rolling direction. The strips were annealed at 400°C for 2 h to relieve internal stresses. Then, the strips were uniaxially strained to various degrees in the range of 1–4 % to obtain different grain sizes. Finally, the specimens were recrystallized in air at 300°C for 2 h and 630°C for 2 h. To identify the grain structure, chemical etchant is used: 30 ml of HCl, 20 ml of HNO_3, 5 ml of HF, 30 ml of H_2O (etching time is 10 s).

To analyze the dislocation sliding and determine active slip systems, the specimen surface was mechanically polished. The microstructure of the specimen surface was analyzed using a MIM-8 optical microscope and a Jeol JSM-840 scanning electron microscope. The crystallographic orientation

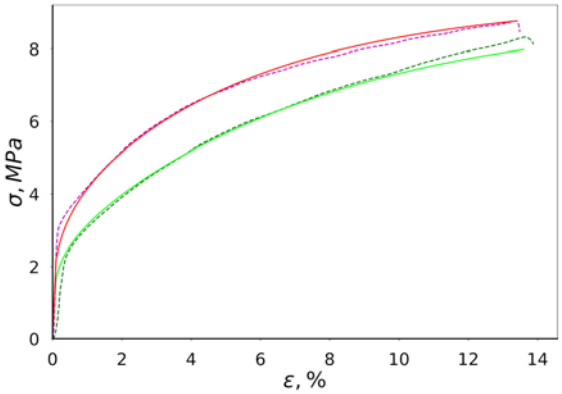

Fig. 2. Experimental (--) and theoretical (-) stress — strain curves of two selected thin sheets of pure aluminum (99.96 %) with two-dimensional pancake-shaped crystals at room temperature and the strain rate of $5 \cdot 10^{-5}$ s^{-1}.

of grains in the specimens in the undeformed state and after tensile deformation was determined by X-ray diffraction (the direct Laue method).

Tensile experiments were performed on Al sheets of various thicknesses in the 110–170 μm range with pancake-shaped crystals with different average grain sizes from 0.2 to 20 mm to obtain stress-strain curves σ(ε) and the curves of stress versus grain size and thickness. The true stresses σ and logarithmic strains ε were calculated as

$$\varepsilon = \ln(l/l_0) \text{ and } \sigma = (F/A_0)(l/l_0),$$

where F is the measured force, l_0 is the initial length, l is the actual length, A_0 is the initial cross-sectional area. The specimens were strained on air until the failure. The strain rate used was $5 \cdot 10^{-5}$ s^{-1}.

3. Results and discussion

3.1. Microstructure, slip pattern and polycrystal deformation

Fig. 1a shows a typical crystallographic orientation of grains of the tensile specimens in the undeformed state. As an example, in each of the six typical specimens, crystallographic orientation of five grains is shown (see also Table). It should be noted that grains with a special orientation practically are not detected. In particular, grains with a cubic orientation which is characterized by the action of four equal slip systems are practically not observed. The grain orientation is random and there is no texture.

Based on the results of studying the surface of deformed samples by optical and

Table 1. Local strain in grains and overall strain of specimens with various thicknesses and average grain sizes until the failure

Specimen	Local strain in grains				
	Grain 1	Grain 2	Grain 3	Grain 4	Grain 5
Specimen I t = 114 μm, d_s = 7.5 mm, ε = 15.1%	10.3%	11.7%	21.7%	11.7%	20.1%
Specimen II t = 159 μm, d_s = 8.9 mm, ε = 13.7%	10.7%	10.8%	14.4%	13.3%	16.8%
Specimen III t = 167 μm, d_s = 4.1 mm, ε = 9.3%	7.1%	10.0%	6.6%	10.4%	9.2%
Specimen IV t = 161 μm, d_s = 5.7 mm, ε = 12.0%	14.5%	14.3%	13.3%	11.1%	8.7%
Specimen V t = 135 μm, d_s = 14.3 mm , ε = 9.9%	6.6%	11.4%	6.6%	10.7%	13.5%
Specimen VI t = 135 μm, d_s = 14.1 mm, ε = 12.0%	15.3%	12.9%	11.1%	10.2%	8.7%

electron microscopy methods performed earlier [15, 16] and in this work, it was found that, in most cases, in grains of two-dimensional polycrystalline aluminum foils under active tensile loading at room temperature, dislocation sliding occurs mainly in one primary slip system. This is apparently due to the absence of constraint in the grain structure and plastic deformation over the thickness of the sample. Fig. 1b (SEM micrograph) shows a typical slip pattern in two adjacent grains near their boundary (vertical traces in two grains correspond to residual rolling marks and coincide with the direction of the tensile axis, ε = 15 %) [15].

In Fig. 2, examples of true stress-strain curves are shown. The dotted green and red lines correspond to the specimen with t = 159 μm, d_s = 8.9 mm and the specimen with t = 142 μm, d_s = 1.4 mm, respectively. According to uniaxial tensile experiments, strain hardening depends on the average grain size and sample thickness.

Table 1 shows the characteristics of plasticity until the failure of random selected five grains in six typical specimens; the crystallographic orientation of the grains in the undeformed state is shown in Fig. 1a. Grains have different local strain, which can be greater or less than the strain of the specimen. Thus, there is an inhomogeneity of strain in the tensile specimens. This inhomogeneity causes a small difference between the experimental and theoretical (see 3.3.1) stress-strain curves in Fig. 2.

3.2. Elements of dislocation theory

3.2.1. Flow stress and dislocation density

An increase in the flow stress with strain is due to the accumulation of dislocations. In the dislocation theory of plasticity, the flow stress τ and dislocation density ρ are related by Taylor's equation [17]:

$$\tau = \alpha\mu b\sqrt{\rho}, \qquad (1)$$

where μ is the shear modulus and b is the magnitude of the Burgers vector of dislocations; α is a numerical constant of the order of unity, which partially depends on the strength of the dislocation/dislocation interaction [10].

As the flow stress τ is determined by (1), its change with strain is due to the dislocation accumulation and dynamic recovery of dislocations. In the Kocks-Mecking model [10–12], the equation for the evolution of ρ:

$$\frac{d\rho}{d\gamma} = k_1\rho^{1/2} - k_2\rho, \qquad (2)$$

where γ is the shear strain. The first term in (2) is associated with the thermal accumulation of moving dislocations. The second term is associated with dynamic recovery of dislocations.

In the present paper, we study uniaxial straining of a thin sheet of pure Al, in which the effect of free surface is important. The free surface serves as both the source and the sink for dislocations. Taking

this into account, the equation (2) can be written in the form presented in [18]:

$$\rho\frac{d\rho}{d\gamma} = \frac{Sn_s}{Vb} + k_1\rho^{3/2} - \frac{1}{bL}\rho - k_2\rho^2. \quad (3)$$

Here S is the surface area of the specimen, and V is its volume; n_s is the density of dislocation sources on the surface; b is the magnitude of the Burgers vector; L denotes the mean-free path of dislocations through the crystallite. The first term in (3) determines the dislocation emission from the surface dislocation sources with the density n_s, and the third term describes the escape of dislocations from the crystal through its surface.

3.2.2. Polycrystal effects

In polycrystalline materials, grain boundaries are important obstacles to slip. Grain boundaries can influence on strain hardening by an additional contribution to the accumulation rate so that (2) transforms to

$$\frac{d\rho}{d\gamma} = \frac{1}{bd} + k_1\rho^{1/2} - k_2\rho, \quad (4)$$

where d is the average grain size [12]. The first term in (4) describes the effect of grain boundaries in bulk polycrystals which can be considered as three-dimensional formations of crystals with $t >> d$.

Thin plates with one grain in thickness are two-dimensional formations of crystals in the form of pancakes ($d_s >> t$) with two free surfaces. Such specimens have only "vertical" grain boundaries, i.e. grain boundaries that are approximately perpendicular to the specimen surface, which obstruct dislocation movement [2, 3]. The deformation will occur in such a way that the central part of the crystal will be more free for the movement of dislocations than the regions of grain boundaries. Thus, the grains of a thin plate with two free surfaces are composed of a softer central part and harder regions near the grain boundaries [1, 2]. Pile-up of dislocations occurs in the harder regions at the grain boundaries, while inside softer grains, dislocations emerge through free surfaces. Indeed, electron microscopic studies of the dislocation structures show a difference in the dislocation structure for core and surface regions of specimens with a different number of grains in thickness [1, 3, 9].

As in bulk metals, grain boundaries an important obstacle to the movement of dislocations in thin films, foils, and plates. Dislocation movement is impeded by grain boundaries throughout the bulk of the sample, if $t >> d$, so that the numerator in the first term in (4) is equal to one. If we now consider a thin plate with $d_s >> t$, then this numerator may be written as:

$$\lambda_h = \frac{V_h}{V_h + V_s}, \quad (5)$$

where λ_h is the volume fraction of the hard boundary region, V_h is the volume of the hard boundary region, V_s is the volume of the soft core region [13]. Therefore equation (3) takes the form

$$\rho\frac{d\rho}{d\gamma} = \frac{\lambda_h}{bL}\rho + \frac{Sn_s}{Vb} + k_1\rho^{3/2} - \frac{1}{bL}\rho - k_2\rho^2. \quad (6)$$

Here, the condition $d = L$ for a thin plate specimen with $d_s >> t$ is taken into account in the first term. It should be noted that equation of the form (6) without the third term and with another coefficient in the first term was used in [4] for theoretical analysis of the effect of reduction in the strength and deviation from the Hall-Petch relationship in fine-dimensional microcrystalline and nanocrystalline specimens of fcc metals. According to [4], the third term could be ignored in (6) because the mechanism of dislocation multiplication on forest dislocations breaks down in a nanocrystalline material with a grain size of $d <$ 1–10 μm. In [4], the first term was written as $(\beta/bd)\rho$. Here β is the relative fraction of grains, which contributes to the grain boundary strengthening. It depends on the ratio between the size factors d and t. The relative fraction of grains is given by $\beta = 1-\Delta S_{cs}/S_{cs}$ [2, 4], where ΔS_{cs} is the total surface area of the surface grains in the cross section of the specimen, S_{cs} is the cross sectional area. In this paper, we use equation (6) to study of grain-size and specimen thickness effect and kinetics in an uniaxially strained thin Al plate with $d_s >> t$.

Taylor assumed that the strain increment is the same for all grains so that

$$Md\varepsilon = d\gamma, \quad (7)$$

where M is the Taylor factor [19]. Equalization of internal and external work: $\tau d\gamma = \sigma d\varepsilon$. Here σ is the normal stress, ε is the logarithmic strain. Therefore

$$M\tau = \sigma. \quad (8)$$

Using (1), (7) and (8), equation (6) can be expressed as

$$d\sigma/d\varepsilon = a_1\sigma^{-1} + a_2\sigma^{-3} + a_3 - a_4\sigma^{-1} - a_5\sigma, \quad (9)$$

where $a_1 = (\alpha\mu b)^2 M^3 \lambda_h / 2Lb$, $a_2 = (\alpha\mu b)^4 M^5 S n_s / 2Vb$, $a_3 = \alpha\mu b M^2 k_1/2$, $a_4 = (\alpha\mu b)^2 M^3/2Lb$, $a_5 = Mk_2/2$. In this study, equation (9) is the basis for the consideration of strain hardening of pure Al specimens with pancake-shaped crystals with two free surfaces at room temperature and a constant strain rate.

3.2.3. Strain hardening

If the coefficients a_1, a_2, a_3, a_4, a_5 of equation (9) are assumed to be constant, then integration of (9) gives

$$A\ln|\sigma - \Sigma_1| + B\ln|\sigma - \Sigma_2| + C\ln|\sigma^2 + \quad (10)$$
$$+ \xi_1\sigma + \xi_2| + D\,\mathrm{arctg}\left(\frac{\sigma + \xi_1/2}{\sqrt{\xi_2 - (\xi_1/2)^2}}\right) + C_0 = \varepsilon.$$

Here, the new parameters A, B, C, D, Σ_1, Σ_2, ξ_1, ξ_2 express the coefficients a_1, a_2, a_3, a_4, a_5. According to (1) and (8), the constant of integration C_0 is determined from the initial condition at $\varepsilon = 0$:

$$\sigma(0) = M\alpha\mu b\rho_0^2, \quad (11)$$

where ρ_0 is the initial dislocation density. Solution of (10) gives the dependence of σ on ε in an implicit form. It will be further used in connection with the study of strain hardening. In particular, using (10) we can calculate the strain-hardening rate $\theta = d\sigma/d\varepsilon$ according to (9).

The coefficients of (9) contain parameters M, λ_h, L which depend on the grain orientation. According to [14], the polycrystalline tensile stress-strain curve $\sigma(\varepsilon)$ may be calculated based on the stress — strain curves for single crystals; this is based on the observed correlations between mechanical behavior of polycrystals and single crystals. In [20], the stress — strain curves $\sigma(\varepsilon)$ are superimposed to take into account the average M-factor of the three groups of grains and weighted in accordance to their volume fractions in the polycrystal. We will consider the problem of polycrystal averaging $\sigma(\varepsilon)$ in the similar way and calculate the stress — strain behavior of two-dimensional polycrystal by averaging the stresses in all grains. A resulted stress-strain curve $\sigma(\varepsilon)$ is calculated as the sum of N contributions for a two-dimensional arrangement of crystals in form of pancakes:

$$\sigma(\varepsilon) = f_1\sigma_1(\varepsilon) + f_2\sigma_2(\varepsilon) + \ldots + f_N\sigma_N(\varepsilon). \quad (12)$$

Here f_i is the volume fraction of the group of grains with the same grain orientation (with the same values M_i, $(\lambda_h)_i$, L_i); $\sigma_i(\varepsilon)$ is determined from the (10) for values M_i, $(\lambda_h)_i$, L_i.

3.3. Analysis of mechanical behavior of thin Al sheets with one grain in thickness

3.3.1. Stress — strain curves

The primary goal of a theory of work hardening is a prediction of the stress-strain curve [12]. In the present work, we analyze uniaxial deformation of pure Al specimens with pancake-shaped crystals with an average grain size of $0.2 < d_s < 20$ mm and a thickness of $0.05 < t < 1$ mm at room temperature and a constant strain rate. Experimental data shows that in many cases, slip predominantly occurs in a single slip system within a grain; therefore, we take into account only one active slip system in the calculations. We believe that our approach is relevant for uniaxial deformation of thin Al sheets with pancake-shaped crystals. In all calculations using (9)–(12), it is assumed that

$$\frac{S}{V} = \frac{2}{t} + \frac{2}{w} \quad (13)$$

for specimens with a rectangular cross section (if $t \ll \omega$ then $S/V \approx 2/t$),

$$L = \frac{t}{\cos\varphi}, \quad (14)$$

$M = 1/m$ [4], where m is the Schmid factor for an active slip system in a grain, φ is the angle between the slip direction and the "vertical" direction in the specimen. For aluminum we use $\mu = 27$ GPa, $b = 0.286$ nm, and also $n_s = (0.1\text{–}0.2)\cdot 10^{12}$ m^{-2}, $k_1 = 10^{-2}/b$, $k_2 = 17$, $\alpha = 0.32$ which correlates with [18, 21].

Often the shape of the grains is chosen such that a regular hexagon is obtained in the cross section of the grain by the surface of the sample. The problem with the analysis is that the volume fraction of the hard boundary region λ_h depends on the hexagon orientation relative to the tension axis. All possible orientations of a regular hexagon are contained within a circle with a diame-

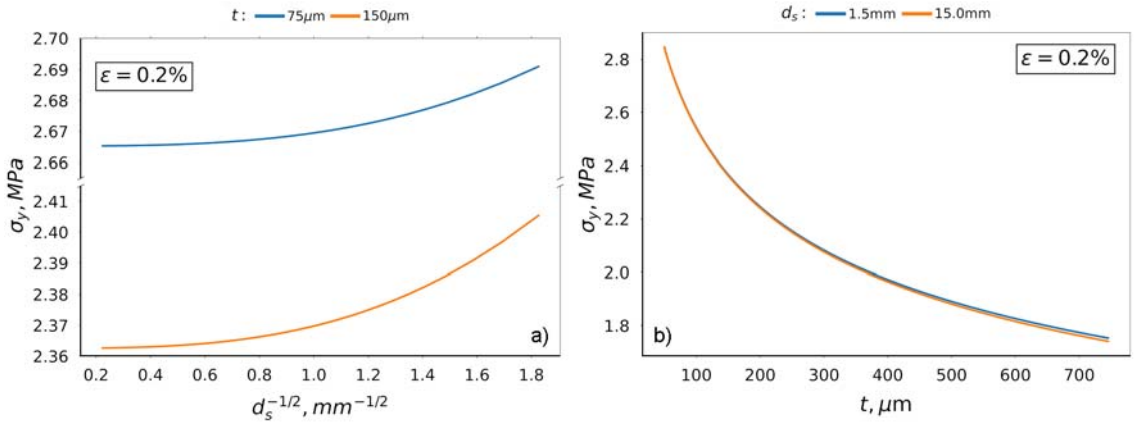

Fig. 3. Dependences of initial yield stress σ_y on average grain size $d_s^{-1/2}$ for thicknesses 75 μm and 150 μm (a); and on thickness t for average grain sizes: 1.5 mm and 15 mm (b).

ter d_s circumscribed around it. Therefore, we will assume that the grains have a cylindrical shape which gives a circle of diameter d_s in the cross section of the grain by the "horizontal" surface of the thin plate specimen. Then λ_h can be calculated analytically:

$$\lambda_h = 2\,\frac{\sqrt{1-\chi^2}(2+\chi^2)/3 - \chi\arccos\chi)}{\pi(1-\chi)} \quad (15)$$

where $\chi = 1 - 2\tan\psi/(t/d_s)$, ψ is the angle between the slip plane in the grain and the "vertical" direction (normal direction) in the specimen with pancake-shaped crystals.

According to [21–24], grain boundaries are assumed to act as sources of dislocations. The dislocations emerge from the grain-boundary ledges. Let δ be the ledge density (the number of ledges per unit length of a grain boundary [23]). Then the number of dislocation sources in the grain boundary is expressed by the relation: $N = S_{GB}\delta^2/2$. Here S_{GB} is the grain boundary area and the factor 1/2 arises from the fact that each boundary is shared by two grains [21, 22]. The total length of dislocations emerging from the grain boundary during yielding is NL_0; where L_0 is the length of dislocations emerging from each source. Therefore the initial density of dislocations is $\rho_0 = S_{GB}\delta^2 L_0/2V_G$, where V_G is the grain volume. In [21, 22], for a spherical grain with a diameter d: $\rho_0 = 3\delta^2 L_0/d$. As noted above, we will assume that the grains have a cylindrical shape with a diameter d_s and a height $H = t$ for thin plates with one grain in thickness. In this case,

$$\rho_0 = \frac{2\delta^2 L_0}{d_s}. \quad (16)$$

In [21], the value $3\delta^2 L_0 b = (1–2)\cdot 10^{-3}$ was used in calculations for aluminum. So we will assume that $2\delta^2 L_0 b = 10^{-3}$ in (16), and therefore, $\rho_0 = 10^{-3}/bd_s$.

Fig. 2 shows the stress — strain curves for specimens of thin sheets of pure aluminum (99.96 %) with pancake-shaped crystals with only one grain in thickness. The dotted and solid lines correspond to the experimental data and calculations by formulas (10–16), respectively. The calculation results are in good agreement with experimental data.

3.3.2. Grain-size and specimen thickness effects in the uniaxial straining of thin Al sheets

The mechanical behavior of polycrystals depends both on the grain size and on the thickness of plate specimens and films [2–4, 9]. The effects of grain size and specimen thickness in the uniaxial straining of thin Al sheets with pancake-shaped crystals at room temperature and a constant strain rate can be explained by accumulation and recovery of dislocations according to equations (6), (9) and solutions (10–16). The grain-size effect is described by the coefficient in the first term in (6) and (9), which depends on the average grain size d_s (see (15)). In addition, the constant of integration C_0 in (10) is determined by the initial dislocation density ρ_0 according to (11), which is inversely proportional to d_s (16). The thickness effect is described by the coefficients in the first, second and fourth terms (see (13–15)). In (6) and (9), the first and second terms are associated with an increase in the dislocation density with strain, and the fourth term is associated with a decrease in

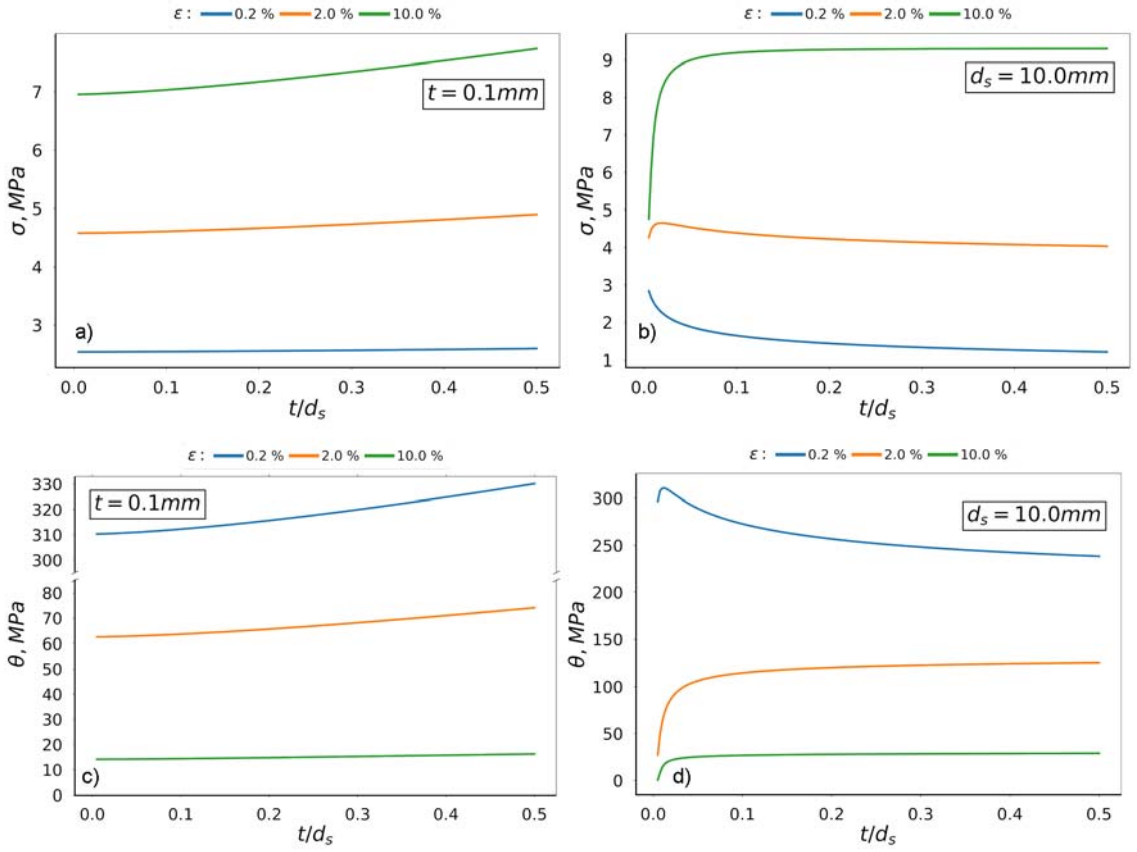

Fig. 4. Dependences of the flow stress σ (a, b) and the strain-hardening rate θ (c, d) on the ratio t/d_s with fixed thickness (a, c) and fixed average grain size (b, d) for various strain levels: 0.2 %, 2 % and 10 %.

the dislocation density with strain. The grain-size (d_s) and specimen thickness (t) effects are discussed below based on calculations using formulas (10–16).

In the early stages of deformation, grain boundaries are important obstacles to moving dislocations. The dependence of initial yield stress σ_y on average grain size d can be expressed according to the well-known Hall-Petch relationship [7, 8]:

$$\sigma_y = \sigma_0 + kd^{-1/2}, \qquad (17)$$

where σ_0 and k are structure-dependent constants. In thin Al sheets with one grain in thickness, there is a deviation from the Hall-Petch relationship. According to calculations in the present study, the dependence of the initial yield stress σ_y on the average grain size d_s is non-linear (Fig. 3a), and instead of expression (17), it is approximated by another power function:

$$\sigma_y = \sigma_0 + k(t)d_s^{-3/2}, \qquad (18)$$

with the essential feature that the coefficient k increases with increasing thickness t. This increase of the coefficient k was experimentally observed in [2] at a logarithmic strain of 0.1.

In [25], a power law of the form $\sigma = \sigma_0 + kd^n$ is discussed. According to several studies, the grain-size exponent should be something other than −1/2. For example, n was −1/3 for the fcc metals and ranged from −1/2 to −0.9 for the bcc metals, or $n = -1/4$ or $n = -1$. Our result $n = -3/2$ differs significantly from these values. It should be noted that the parameters d and d_s have different meanings. Pancake-shaped crystals are not equiaxed in three dimensions. On the specimen surface, grain dimensions have to be characterized by a size parameter d_s, whereas the dimension for thickness is given by a size parameter d_t. For pancake-shaped crystals, $d_s >> d_t = t$, so d_s is taken as a representative grain size parameter [2]. In bulk polycrystals, the mean-free path of dislocations is limited by the grain size d. For thin plates with $d_s >> d_t$, the mean-free

path of dislocations L is determined by Eq. (14) and does not depend on d_s. Pile-up of dislocations at the vertical grain boundaries in the harder grain boundary regions and escape of dislocations through the free surfaces in the softer grain interiors are observed. The first term in (6) describes the effect of grain boundaries in thin plates with pancake-shaped crystals. The grain size dependence is only due to the vertical grain boundary regions. The role of the parameter d_s is that as d_s decreases, the volume of the hard vertical grain boundary region V_h and the volume fraction of the hard vertical grain boundary region λ_h (5) increases according to (15) (the grain-size effect).

In Al sheets with pancake-shaped crystals with various average grain sizes, initial yield stress decreases with increasing thickness (Fig. 3b). A similar trend was found in [4]. Such dependence $\sigma_y(t)$ is due to the fact that at the early stage of deformation, the second term dominates in (6), i.e. the dislocation emission from the surface dislocation sources (the free surface effect) plays a dominant role in mechanical behavior.

With an increase in strain ε, the character of the stress dependence on the grain size and thickness of the specimens changes. With further uniaxial deformation, the relative role of surface dislocation sources is significantly weakened and the relative role of the multiplication of dislocations on forest dislocations and the annihilation of dislocations increases. The third and fifth terms in Eq. (6), which are associated with the thermal accumulation of moving dislocations and with dynamic recovery of dislocations, respectively, begin to dominate. As a result, as the deformation significantly exceeds 0.2 %, an increase in stress with a decrease in grain size becomes more pronounced (Fig. 4a), and the decreasing dependence of stress on thickness turns into the increasing dependence (Fig. 4b). In addition, Fig. 4a and Fig. 4b show the dependence of the flow stress on the ratio t/d_s, as was done in [2, 9] for various strain levels at fixed thickness and fixed grain size, respectively. According to [2], the flow stress is only dependent on t/d_s and not on the absolute thickness or average grain size; but as can be observed (see Fig. 4a, b), the flow stress depends not only on the ratio t/d_s, but also on the parameters t and d_s separately.

Analysis of the dependences of the strain-hardening rate $\theta = d\sigma/d\varepsilon$ (9) on the ratio t/d_s for various strain levels at a fixed thickness (Fig. 4c) and fixed grain size (Fig. 4d), respectively, also shows that θ depends on each of the parameters t and d_s separately, and not only from their ratio. In the early stages of deformation, the strain-hardening rate θ increases with decreasing grain size and specimen thickness. With an increase in strain, the value of θ decreases, while the dependence of θ on the grain size becomes weaker, and the dependence of θ on the thickness turns from decreasing to increasing. Thus, the observed dependences of the flow stress and the strain-hardening rate can be explained by competition between the accumulation and annihilation of dislocations, proceeding from the equations of the kinetics of dislocations (6) and (9).

4. Conclusions

Taking into account the feature of the structure and geometric shape of flat two-dimensional polycrystalline Al specimens, the coefficients of the kinetic equation which describes the evolution of the dislocation density under uniaxial tension at a constant strain rate at room temperature have been calculated. Based on the equations of dislocation kinetics, the stress — strain curve σ(ε) for flat Al specimens with a "pancake" grain structure was calculated theoretically. The calculation results are in good agreement with the experimental data for Al specimens (99.96 %) with various thicknesses in the range of 110–170 μm and different average grain sizes from 0.2 to 20 mm.

The kinetic consideration of the processes of multiplication and annihilation of dislocations made it possible to found the dependences of the flow stress and the strain-hardening rate on the average grain size and specimen thickness in the ranges $0.2 < d_s < 20$ mm and $0.05 < t < 1$, respectively. The dependence of the coefficients of the kinetic equations on the grain size and specimen thickness explains the d_s- and t-size effects studied in the present work.

For the initial yield stress, an approximate Hall-Petch-type relation is obtained, in which the coefficient at the power function of the grain size depends on the specimen thickness, and the exponent of this function is −3/2. The initial yield stress decreases with increasing specimen thickness. At strains significantly exceeding 0.2 %, an increase in stress with a decrease

in grain size becomes more and more pronounced, and a decreasing dependence of stress on thickness turns into an increasing dependence. In the early stages of uniaxial deformation, the strain-hardening rate θ increases with decreasing grain size and specimen thickness. With an increase in strain, the value of θ decreases, while the dependence of θ on the grain size becomes weaker, and the dependence of θ on the thickness changes from decreasing to increasing. The changes in the course of the considered dependences with an increase in strain are explained by the fact that at different stages of deformation, different terms in kinetic equations that describe dislocation accumulation and annihilation of dislocations are dominated.

References

1. H.-J.Leea, P.Zhang, J.C.Bravman, *J. Appl. Phys.*, **93**, 1443 (2003).
2. P.J.Janssen, T.H.de Keijser, M.G.Geers, *Mater. Sci. Eng.*, **A 419**, 238 (2006).
3. C.Keller, E.Hug, R.Retoux, X.Feaugas, *Mechan. Mater.*, **42**, 44 (2010).
4. G.A.Malygin, *Phys. Solid State*, **54**, 559 (2012).
5. K.M.Davoudi, J.J.Vlassak, *J. Appl. Phys.*, **123**, 085302 (2018).
6. T.R.Bielera, R.Alizadeh, M.Pena-Ortega, J.Llorca, *Intern. J. Plasticity*, **118**, 269 (2019).
7. E.O.Hall, *Proc. Phys. Soc. B.*, **64**, 747 (1951).
8. N.J.Petch, *J. Iron Steel Inst.*, **174**, 25 (1953).
9. S.Miyazaki, K.Shibata, H.Fujita, *Acta Metall.*, **27**, 855 (1978).
10. U.F.Kocks, H.Mecking, *Acta Metall.*, **29**, 1865 (1981).
11. Y.Estrin, H.Mecking, *Acta Metall.*, **32**, 57 (1984).
12. U.F.Kocks, H.Mecking, *Progr. Mater. Sci.*, **48**, 171 (2003).
13. E.E.Badiyan, A.G.Tonkopryad, Ye.V.Ftomov, O.V.Shekhovtsov, *Functional Materials*, **26**, 484 (2019).
14. N.Hansen, X.Huang, *Acta Mater.*, **46**, 1827 (1998).
15. E.E.Badiyan, A.G.Tonkopryad, O.V.Shekhovtsov et al., *Functional Materials*, **22**, 396 (2015).
16. Ye.V.Ftomov, *J. V.Karazin Kharkiv National University, Ser. "Physics"*, **34**, 25 (2021).
17. G.I.Taylor, *Proc. Roy. Soc. A.*, **145**, 362 (1934).
18. G.A.Malygin, *Phys. Solid State*, **52**, 49 (2010).
19. G.I.Taylor, *J. Inst. Metals*, **62**, 307 (1938).
20. X.Huang, A.Borrego, W.Pantleon, *Mater. Sci. Engin. A*, **319–321**, 237 (2001).
21. G.A.Malygin, *Phys. Solid State*, **49**, 1013 (2007).
22. J.C.M.Li, T.Chou, *Metal. Trans.*, **1**, 1145 (1970).
23. E.S.Venkatesh, L.E.Murr, *Mater. Sci. Eng.*, **33**, 69 (1978).
24. E.V.Esquivel, L.E.Murr, *Mater. Sci. Eng. A*, **409**, 13 (2005).
25. Z.C.Cordero, B.E.Knight, C.A.Schuh, *Intern. Mater. Rev.*, **61**, 495 (2016).